Hindered Rotational Diffusion and Rotational Jumps of Single Molecules

T. Ha,[1] J. Glass,[1,2] Th. Enderle,[1,*] D. S. Chemla,[1,2] and S. Weiss[1]
[1]*Materials Sciences Division, Lawrence Berkeley National Laboratory, 1 Cyclotron Road, Berkeley, California 94720*
[2]*Department of Physics, University of California at Berkeley, Berkeley, California 94720*
(Received 19 September 1997)

We extended the sensitivity of fluorescence polarization anisotropy measurements to the single molecule level by studying the polarization response of single fluorophores rapidly rotating in liquid. Comparison with a simple model calculation allows us to obtain information on the hindered motion as well as on the rotational diffusion in the presence of specific molecular interactions. We also observed rotational jumps between surface-bound and unbound states and show that they are, similar to jumps to long dark states, photoactivated. [S0031-9007(98)05503-3]

PACS numbers: 33.15.Kr, 33.50.–j, 33.80.–b

Among the most exciting possibilities opened up by the recent advances in room-temperature fluorescence spectroscopy of single molecules [1–16] is the prospect of observing conformational changes of macromolecules undergoing biochemical reactions. Two properties of a single fluorescent probe attached to a macromolecule can be exploited in a way which is not possible in an ensemble study. The first is the high sensitivity of the fluorophore to factors in its local environments such as quenchers. The second is its unique transition dipole, which can be interrogated by polarized excitation/emission. Conformation change can be detected by measuring distance changes between two sites on the macromolecule, via single-pair fluorescence resonance energy transfer [10], or by detecting changes in the dipole orientation of a rigidly attached probe [12,17,18], or by their combination.

Light absorption by a fluorescent molecule is proportional to $(\vec{E} \cdot \vec{\mu})^2$ or to $\cos^2(\theta)$ where θ is the angle between the electric field $\vec{E}$ and the dipole moment $\vec{\mu}$. By continuously rotating $\vec{E}$, this cosine dependence was recently shown [12,19] on single molecules. Concurrent recording of polarization response of single molecules can make a distiction between rotational jumps and various other dynamical events such as spectral diffusion and dark states [4,12]. In liquids, rotational dynamics become more prominent, and it is even more important to clearly separate out the rotational part from other processes.

In this Letter we use polarization anisotropy with continuously rotated excitation angle to measure rotational dynamics of single fluorophores in liquid. In contrast to conventional steady-state ensemble fluorescence polarization anistropy, it provides information on the hindered motion of the fluorophore in addition to rotational diffusion.

A Texas Red fluorophore was covalently linked to a short DNA molecule by a flexible carbon chain. The DNA-fluorophore complexes were adsorbed on a glass surface [10] with a density of 0.5 molecules/μm^2 and excited, one at a time, by a tightly focused laser spot ($\sim$0.4 μm). In contrast to a previous study under dry conditions [12], fluorescent molecules under aqueous buffer were frequently detached from the surface and rapidly rotated around the carbon tether. Since the fluorophores were anchored to the substrate through the DNA molecule, they could not diffuse away from the excitation volume. This arrangement is most suited for the investigation of rotational diffusion kinetics of single molecules. It is worth noting that many *in vitro* biological experiments are performed under similar conditions, where fluorescent labels are used to probe biological macromolecules at water-solid interfaces.

Automatic search was employed to locate the molecules at the center of the laser spot [20]. The excitation laser light was linearly polarized and the polarization angle was repeatedly swept over 120°. The fluorescence emission intensities were split by a polarizing beam splitter (PBS) to two components I_s and I_p ($\hat{s}$ and $\hat{p}$ are orthogonal polarization angles defined relative to the PBS) and recorded by two detectors (see Fig. 1).

Typical single molecule data are shown in Fig. 2. Figure 2(a) shows raw data of simultaneously obtained emission time traces of a rapidly rotating molecule. The single molecule nature of the signal is evident from the abrupt photobleaching. Figure 2(b) shows the same data as in Fig. 2(a), background subtracted and 11 periods averaged. The x axis is converted to the laser polarization angle, θ, measured relative to the $\hat{p}$ polarization. Figures 2(c), 2(d), and 2(e) show similarly processed data for another three molecules. In general, both I_s and I_p follow a $\cos^2(\theta)$ curve with a nonzero base line. The relative phase between I_s and I_p as well as their modulation depth is a very sensitive function of the molecular rotation characteristics. The excitation is most effective when $\vec{\mu} \| \vec{E}$, and the polarization of the emitted light is parallel to $\vec{\mu}(t)$ at the moment of emission. For example, in the case of an immobilized fluorophore, the in-plane dipole is determined from the absolute phase of either I_s or I_p (which have the same phase) [12]. For a freely rotating fluorophore, with a rotational diffusion slower or comparable to the emission lifetime, the emission polarization will mostly follow

 © 1998 The American Physical Society

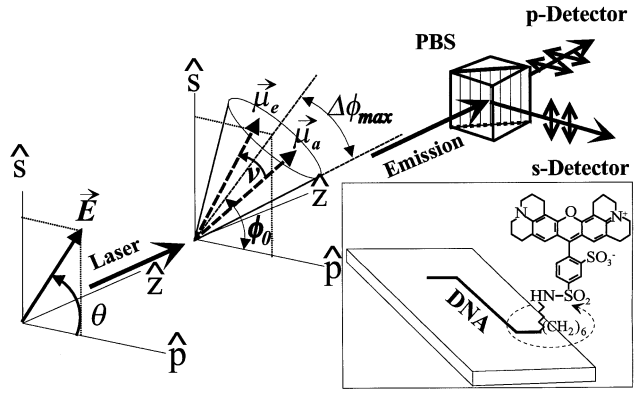

FIG. 1. Experiment schematics: $\vec{E}$—excitation field, making an angle θ relative to $\hat{p}$. $\hat{z}$ is the propagation direction for the exciting field and the collection axis for the fluorescence emission. $\vec{\mu}_a$ and $\vec{\mu}_e$ are the molecular dipole moments for absorption and emission. υ represents the rotational diffusion during the excited state lifetime. The dipole moment is constrained to a cone with a center angle ϕ_0 and a half cone angle $\Delta\phi_{\max}$. The collected emission is split by the PBS and the two signals, I_s and I_p, are simultaneously recorded. The inset shows the chemical structure of the dye-DNA complex and the linker region.

$\vec{E}(t)$, i.e., if $\vec{E}\|\hat{s}$, $I_s > I_p$ and if $\vec{E}\|\hat{p}$, $I_s < I_p$, resulting in a (180°) phase difference between the two signals. In the case of a hindered rotation in a limited cone angle, the phase shift between the two signals will take an intermediate value between 0° and 180°. We show below that this qualitative discussion can be put on a firm basis and lead to quantitative information about the degree of hindered rotation and the rotational diffusion rate.

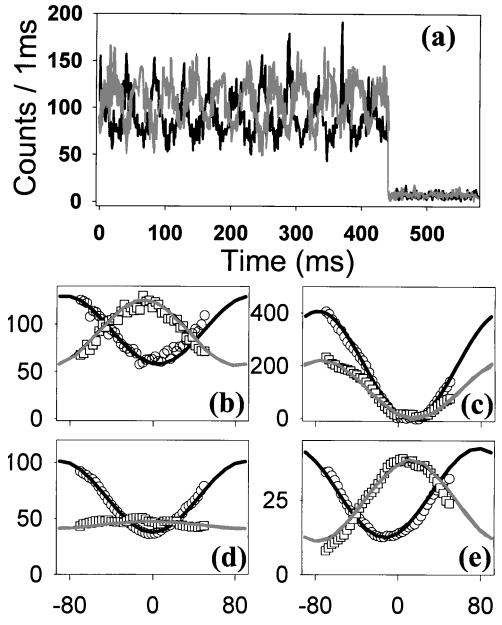

FIG. 2. (a) Simultaneously recorded I_s (black line) and I_p (gray line) of a molecule rapidly rotating in liquid. (b) The data in (a) after time averaging and background subtraction. Circles for I_s and squares for I_p. Best fits according to the model described in the text are shown. (c), (d), and (e) are results on three other molecules.

The single fluorophore is modeled by a dipole moment rapidly rotating within a cone. In principle, it is possible to numerically solve the rotational diffusion equation with the boundary condition of the cone for 3D rotation. However, to make the calculation simpler, we consider here the case of a dipole rotating in the plane with reflecting boundary conditions [21]. Since the measurement is sensitive only to the in-plane component of the dipole, the approximation is quite good as long as the projection to the plane is properly accounted for (see below). The dipole is allowed to rotate in the $\hat{s}$-$\hat{p}$ plane and makes an angle ϕ with $\hat{p}$ (see Fig. 1). It is rotating around the angle ϕ_0, with a half cone angle, projected to the plane, of $\Delta\phi_{\max}$: $\phi_0 - \Delta\phi_{\max} < \phi < \phi_0 + \Delta\phi_{\max}$. It is further assumed that (i) the dipole can be found anywhere within the cone with identical probabilities [result of the reflecting boundary conditions, Eq. (3)], and that (ii) $\vec{\mu}_a\|\vec{\mu}_e$ (absorbtion and emission dipoles are collinear) in the absence of rotational diffusion. The probability distribution function to find the dipole at an angle ϕ' at time t after excitation at $t = 0$ and angle ϕ is $\upsilon(\phi, \phi', t)$, given as a solution of the following diffusion equation:

$$\frac{\partial \upsilon(\phi, \phi', t)}{\partial t} = D^* \frac{\partial^2 \upsilon(\phi, \phi', t)}{\partial^2 \phi'}, \tag{1}$$

where D^* is the effective rotational diffusion coefficient. Solution for υ is obtained from the initial condition:

$$\upsilon(\phi, \phi', t = 0) = \delta(\phi - \phi') \tag{2}$$

and reflecting boundary conditions:

$$\left.\frac{\partial \upsilon}{\partial \phi'}\right|_{\phi' = \phi_0 - \Delta\phi_{\max}} = 0, \qquad \left.\frac{\partial \upsilon}{\partial \phi'}\right|_{\phi' = \phi_0 + \Delta\phi_{\max}} = 0. \tag{3}$$

I_s and I_p, for a given excitation polarization angle θ, are evaluated by

$$I_s \propto \int_0^\infty \int_{\phi'} \int_{\phi} [\vec{E}(\theta) \cdot \vec{\mu}(0)]^2 \times [\hat{s} \cdot \vec{\mu}(t)]^2 \upsilon f(t)\, d\phi'\, d\phi\, dt \tag{4}$$

and similarly for I_p. The absorption probability is given by $[\vec{E}(\theta) \cdot \vec{\mu}(0)]^2$, where $\vec{\mu}(0)$ is the dipole moment orientation upon excitation at $t = 0$. The emission probability along $\hat{s}$ is $[\hat{s} \cdot \vec{\mu}(t)]^2$ and similarly for $\hat{p}$, where $\vec{\mu}(t)$ is the dipole moment at time t. Hindered rotational diffusion is expressed as $\upsilon(\phi, \phi', t)$ and the lifetime effect is accounted for by $f(t) = e^{-t/\tau}/\tau$, where τ is the emission lifetime. For angular integration, the rotational time scale is assumed to be much faster than the data acquisition time T. Temporal integration accounts for the steady-state nature of the measurement, and the calculation is repeated for each θ.

The resulting calculated signals, $I_s(\theta)$ and $I_p(\theta)$, are plotted in Fig. 3. The product $D^*\tau$ is a measure of the rotational diffusion rate and $\Delta\phi_{\max}$ represents the degree

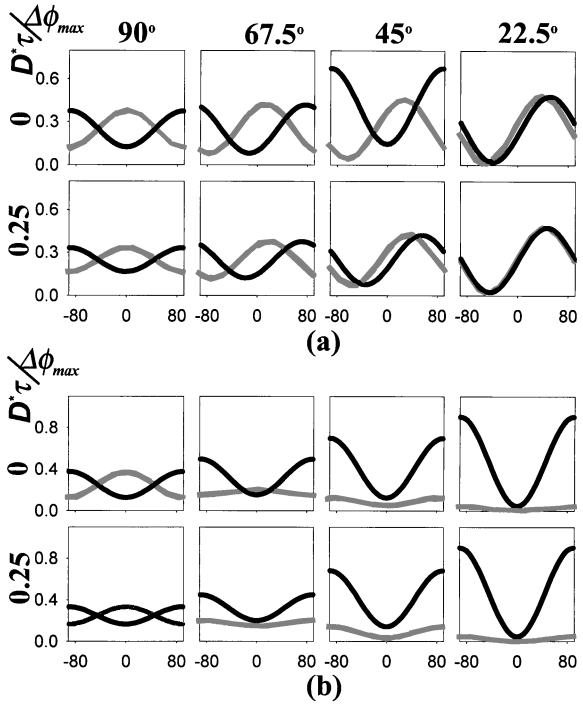

FIG. 3. Model calculation for $I_s(\theta)$ (black line) and $I_p(\theta)$ (gray line) for given $D^*\tau$, ϕ_0, and $\Delta\phi_0$. ϕ_0 is 45° for (a) and 90° for (b).

of allowed rotation. Note that $D^*\tau \cong 0$ for rotation much slower than τ, and $D^*\tau \gg 1$ for very fast rotation. Also, $\Delta\phi_{\max} = 0$ for a fixed dipole and $\Delta\phi_{\max} = 90°$ for free rotation. The results are arranged in a table form, where plots of I_s and I_p are displayed for a few selected values of $D^*\tau$, $\Delta\phi_{\max}$, and ϕ_0. The top row in Fig. 3(a) illustrates the effect of the rotational hindrance. Both the relative phase and the modulation depth change as $\Delta\phi_{\max}$ changes from free rotation ($\Delta\phi_{\max} = 90°$) to a fixed dipole ($\Delta\phi_{\max} = 0$). The second row illustrates the effect of faster rotation. With the help of the tables of Fig. 3 and a fitting procedure (which will be described elsewhere, fits shown in Figs. 2(b)–2(e), we can unambiguously determine ϕ_0, $\Delta\phi_{\max}$, and $D^*\tau$.

All 11 rotating molecules examined could be fit in a similar manner and the resulting distributions of $\Delta\phi_{\max}$ and $D^*\tau$ are shown in Fig. 4. The steric hindrance due to neighboring chemical groups, determined by the geometrical structure of the DNA molecule and the surface, can restrict $\Delta\phi_{\max}$ to a value $<90°$, as observed for 11 studied molecules. Because of residual birefringence in the optics, it is not possible to distinguish between completely immobilized molecules and slightly dithering molecules ($0 < \Delta\phi_{\max} < 20°$). However, the absence of rotating molecules with $\Delta\phi_{\max} < 50°$ indicates that the molecules are rapidly rotating with relatively small perturbation once detached.

Conventional fluorescence polarization anisotropy measurement on an ensemble of the same DNA-fluorophore complexes in solution [10] yielded anisotropy $r = 0.17$

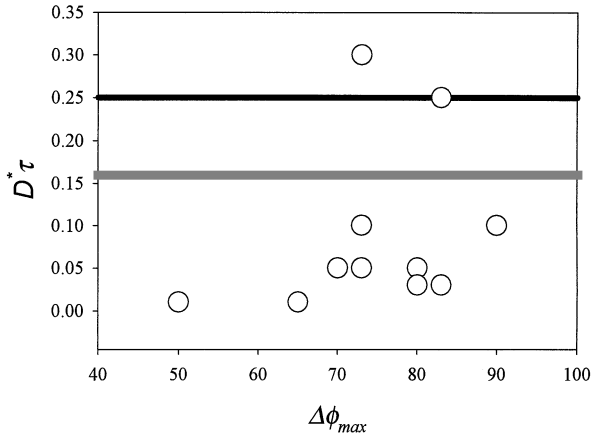

FIG. 4. Values of $D^*\tau$ and $\Delta\phi_0$ for 12 rapidly rotating molecules (circles). The two horizontal lines indicate $D^*\tau$ for the ensemble measurement in 3D (black line) and corrected for projection to the plane (gray line).

and corresponding rotational diffusion parameter of $D\tau = 0.25$, where D is the 3D rotational diffusion coefficient. In solution, the free, but relatively heavy DNA molecule is quasistationary during the emission lifetime, so the local motion of the fluorophore around its attachment point to the DNA is the main cause of the Brownian depolarization. It is therefore possible to directly compare the ensemble measurements with those of the single immobilized DNA-fluorophore complexes on the glass-water interface. The ensemble result of $D\tau = 0.25$ is shown as a black line in Fig. 4. Most of the data points lie below this line because (i) D^* is smaller than D by a projection factor of up to $2/\pi$. The correction for this projection factor is replotted with a gray line in the figure; (ii) the rotational diffusion of fluorophores is further slowed down due to the interaction with the surface.

The data in Figs. 2(b) and 2(c) are indicative of a freely rotating and a fixed fluorophore, respectively. However, many fluorophores displayed a mixed behavior, where approximately half of the time they were fixed to the surface and half of the time they freely rotated. About 40% of them underwent at least one rotational jump (defined as an abrupt change in ϕ_0 and/or in $\Delta\phi_{\max}$). The time sequence in Fig. 5(a) shows seven consecutive rotational jumps experienced by a single molecule. Surprisingly, as seen in Fig. 5 for this particular molecule, and also for many others, molecules are repeatedly readsorbed to the surface with the same ϕ_0 (with arbitrary distribution of ϕ_0 among molecules). These repeated visits to the same fixed state suggest a favorable binding geometry to the DNA or to the surface.

In addition to rotational jumps, we also observe long (>10 ms) dark states that are momentary cessation of the emission up to a few seconds. Dark states, or "blinking," have been observed for many different systems [2,15,16,22,23]. Although the origin of these dark states is not known, it is possible that it is due to a photogenerated, nonfluorescent twisted conformation [24]. To see if the

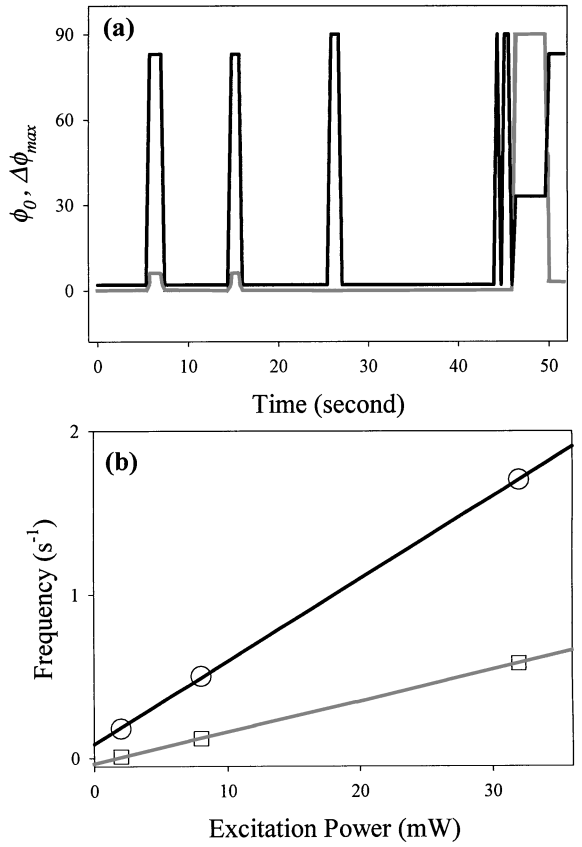

FIG. 5. (a) Time sequence of seven consecutive rotational jumps experienced by a single molecule. ϕ_0 (gray line) and $\Delta\phi_{\max}$ (black line) are plotted as function of time. (b) Rotational jump frequency (circles) and jumping frequency to dark states (squares) as functions of excitation power. Linear regression fits are also shown.

rotational jumps and dark states are light driven or spontaneous, measurements were made for three different excitation powers P of 2, 8, and 32 μW. The data were compiled for a total of 60 molecules, 20 molecules for each P. The total time of emission, T_e, the number of rotational jumps, N_r, and the number of jumps to dark states, N_d, were extracted for each molecule. The rotational jump frequency $f_r = \sum N_r/(\sum T_e)$ and the jump frequency to dark states $f_d = \sum N_d/(\sum T_e)$ were calculated and plotted for each P in Fig. 5(b). Both f_r and f_d are clearly linearly dependent on P, indicating they are photoactivated. Linear regressions to the data reveal that $f_d(0) \cong 0$ but $f_r(0) = 0.09\ s^{-1}$, showing spontaneous rotational jumps at zero P. The total time of emission and the total number of rotational jumps for all 60 molecules were 367 s and 107 jumps, respectively. The number of spontaneous rotational jumps is therefore given by $367 \times 0.09 = 33$, which is about 30% of the total. For 367 s, 4×10^7 photons were emitted. Since there were 74 $(107 - 33)$ photoactivated rotational jumps, it follows that it takes about $4 \times 10^7/75 \cong 5 \times 10^5$ emission cycles for the rotational jump to be activated. In the same span, 35 dark states were observed, and therefore it takes $4 \times 10^7/35 \cong 10^6$ emission cycles to activate jumps to dark states. It is likely that photoactivated rotational jumps as well as dark states are caused by a light-induced conformational change. Such a change can alter the binding strength of the fluorophore to the surface and induce desorption or readsorption. Spontaneous jumps might arise from thermally activated conformational changes and should also be responsible for the much enhanced probability of rapid rotation in liquid. Preliminary data obtained for other fluorophore-DNA complexes in liquid suggest that the equilibrium population in the rapidly rotating state ranges from near zero (CY5) to 100% (tetramethylrhodamine). Specific molecular interaction must be responsible for the differences. We previously reported the correlation between dark states and spectral jumps [25]. In this work, we did not find any correlation between the dark states and the rotational jumps. Distinct conformations and reaction pathways should be responsible for dark states and rotational jumps.

This work was supported by the Laboratory Directed Research and Development Program of Lawrence Berkeley National Laboratory under U.S. Department of Energy, Contract No. DE-AC03-76SF00098.

*Present address: Pharma Preclinical R&D, F. Hoffmann-La Roche Ltd., CH-4070 Basel, Switzerland.

[1] E. Betzig and R. J. Chichester, Science **262**, 1422 (1993).
[2] W. P. Ambrose *et al.*, Phys. Rev. Lett. **72**, 160 (1994).
[3] S. Nie *et al.*, Science **266**, 1018 (1994).
[4] X. S. Xie and R. C. Dunn, Science **265**, 361 (1994).
[5] W. P. Ambrose *et al.*, Science **265**, 364 (1994).
[6] J. K. Trautman *et al.*, Nature (London) **369**, 40 (1994).
[7] Th. Schmidt *et al.*, J. Phys. Chem. **99**, 17 662 (1995).
[8] T. Funatsu *et al.*, Nature (London) **374**, 555 (1995).
[9] J. J. Macklin *et al.*, Science **272**, 255 (1996).
[10] T. Ha *et al.*, Proc. Natl. Acad. Sci. U.S.A. **93**, 624 (1996).
[11] R. D. Vale *et al.*, Nature (London) **380**, 451 (1996).
[12] T. Ha *et al.*, Phys. Rev. Lett. **77**, 3979 (1996).
[13] H. P. Lu and X. S. Xie, Nature (London) **385**, 143 (1997).
[14] R. M. Dickson *et al.*, Science **274**, 966 (1996).
[15] R. M. Dickson *et al.*, Nature (London) **388**, 355 (1997).
[16] D. A. Vanden Bout *et al.*, Science **277**, 1074 (1997).
[17] I. Sase *et al.*, Proc. Natl. Acad. Sci. U.S.A. **94**, 5646 (1997).
[18] J. E. T. Corrie *et al.*, Biophys. J. **72**, A1 (1997); **72**, A52 (1997).
[19] F. Güttler *et al.*, J. Lumin. **56**, 29 (1993).
[20] T. Ha *et al.*, Appl. Phys. Lett. **70**, 782 (1997).
[21] P. Wahl, Chem. Phys. **7**, 210 (1975).
[22] T. Ha *et al.*, Chem. Phys. Lett. **271**, 1 (1997).
[23] M. Nirmal *et al.*, Nature (London) **383**, 802 (1996).
[24] G. Vamosi *et al.*, Biophys. J. **71**, 972 (1996).
[25] T. Ha *et al.*, IEEE J. Sel. Top. Quantum Electron. **2**, 1115 (1996).